Nat Hazards (2017) 87:1525–1543
DOI 10.1007/s11069-017-2828-0

ORIGINAL PAPER

GIS-based flood risk assessment in suburban areas: a case study of the Fangshan District, Beijing

Shanshan Hu[1,2] · Xiangjun Cheng[1,2] · Demin Zhou[1,2] · Hong Zhang[1,2]

Received: 1 August 2016 / Accepted: 13 March 2017 / Published online: 17 March 2017

Abstract Suburban areas have become rapid development zones during China's current urbanization. Generally, these areas are also regional precipitation centers that are prone to flood disasters. Therefore, it is important to assess the flood risk in suburban areas. In this study, flood risk was defined as the product of hazard and vulnerability based on disaster risk theory. A risk assessment index system was established, and the analytic hierarchy process method was used to determine the index weight. The Fangshan District in Beijing, China, which is an example of a typical suburban area undergoing rapid urbanization, was selected for this study. Six factors were considered in relation to hazard, and three factors were considered for vulnerability. Each indicator was discretized, standardized, weighted, and then combined to obtain the final flood risk map in a geographical information system environment. The results showed that the high and very high risk zones in the Fangshan District were primarily concentrated on Yingfeng Street, Xingcheng Street, Xincheng Street, and Chengguanzhen Street. The comparison to an actual flood disaster suggested that the method was effective and practical. The method can quantitatively reflect the relative magnitude and spatial distribution patterns of flood risk in a region. The method can be applied easily to most suburban areas in China for land use planning and flood risk management.

Keywords Flood · Risk assessment · AHP · GIS · Suburban areas

✉ Shanshan Hu
hushanshan@cnu.edu.cn

[1] College of Resource Environment and Tourism, Capital Normal University, 105 West Third Ring Road, Haidian District, Beijing 100048, China

[2] State Key Laboratory of Urban Environmental Processes and Digital Modeling, Capital Normal University, Beijing 100048, China

1 Introduction

Floods have major impacts in many areas of the world (Wells et al. 2016). In China, it is one of the major natural hazards that cause death and millions of dollars of economic losses. The national annual average loss due to flood disasters was approximately 110 billion yuan, which amounts to 2% of the contemporary gross domestic product (GDP) (Zhou and Zhang 2009). In recent years, global warming has caused an increase in the frequency and intensity of extreme rainfall events, which will, in turn, cause more floods in many parts of the world (Alfieri et al. 2015; Ranger et al. 2011; Liu et al. 2011). Furthermore, rapid urbanization has significantly affected the natural environment. Land surface change, population, and wealth concentration have led to a continuous increase in flood losses. China has become extremely urbanized during the last 30 years, particularly in the suburbs of the city (Liu et al. 2015). These suburban areas include new towns and the satellite areas of many large cities. Therefore, assessments of flood hazards, vulnerability, and risk in suburban areas have significant practical implications for urban planning and flood management.

Numerous studies have investigated flood risk assessment in different parts of the world. The assessment methods primarily include geomorphology analysis (Camarasa-Belmonte and Soriano-García 2012), hydrology and hydraulics simulation models (Hsu et al. 2011), flood damage models (Vorogushyn et al. 2012), remote-sensing image extraction (Islam and Sado 2000; Ayalew 2009; Skakun et al. 2014), and statistical analysis of historical data (Wu et al. 2015). These conventional approaches are often limited due to a lack of adequate data and are uneconomic in suburban areas. Many suburban areas in China are located within a transition zone between mountains and plains, particularly in mountainous areas (Tullos et al. 2016). The complex and variable terrain, limited accessibility, scarcity of hydrometeorological data, and inadequate statistical and process-based models make it difficult to conduct flood risk assessment in these areas. A geographical information system (GIS) allows for the storage and efficient processing of data derived from various sources, such as maps, satellite imagery, and land surveys. In addition, GIS provides a powerful spatial analysis function based on predefined criteria, which will improve the precision of risk assessment (Yang 2013; Liao and Sun 2003). Regarding this process, flood risk assessment can be delineated through the integration of multi-dimensional impact factors using a weighted integration method in a GIS environment (Al-Abadi et al. 2016; Zare 2016; Wang et al. 2011).

Several weighting methods have been developed, such as the analytic hierarchy process (AHP), the fuzzy comprehensive evaluation model, the gray target model, principal component analysis, set pair analysis, technique for order preference by similarity to the ideal solution, data envelopment analysis, and the variable sets method (Zou et al. 2013; Lai et al. 2015; Zeng et al. 2012). Among these methods, the AHP method is the most widely used and has proven to be useful in flood risk studies (Siddayao et al. 2014; Zou et al. 2013; Yang et al. 2013; Chen et al. 2011; Elkhrachy 2015). This method has clear practical significance and strong practicability and can realistically reflect all components of a flood disaster system simultaneously. The AHP was selected in this study to assign ranks to each causative flood factor.

The Fangshan District of Beijing, which is one of the key development areas in the future based on Beijing's "Two Axes-Two Belts and Multi-centers" development plan, was chosen as the case study area. The objective of this study is to present a flood risk assessment model for suburban areas. First, a wide range of indicators across

geomorphological, geological, and socioeconomic aspects were chosen, which were spatially dispersed. Then, the AHP was implemented to evaluate these factors, where the data processing was performed in a GIS environment. Lastly, a comparison of the assessment results and an actual flood disaster was conducted to obtain a reasonable evaluation of the proposed approach.

2 Study area and data sources

2.1 Study area

The Fangshan District is located in southwestern Beijing between 115°25′–116°15′E and 39°30′–39°55′N (Fig. 1). It is located in the transition zone between the North China plain and the Taihang Mountains. The total area of the district is 1990 km^2. The western and northern areas contain mountains and hills, and the eastern area is a plain. The maximum elevation difference is 2000 m. The Fangshan District has a continental monsoon climate and falls within the north temperate zone. The annual mean temperature is approximately 10–12 °C, and the multi-year average precipitation is approximately 655 mm. The rainy season spans from June to August and accounts for 85% of the annual total precipitation. Precipitation is intense during this time and includes abundant rainstorms and hail. There are numerous rivers in the study area, including the Dashi River, the Juma River, and the Xiaoqing River. Because the rainy season in the Fangshan District is relatively short and the area is characterized by large differences in elevation, the Fangshan District is prone to flash floods.

The Fangshan District is part of Beijing's western development zone and is a key node in Beijing's development plan. The district includes modern manufacturing and material industries (the petroleum and chemical industry, new-type building material), as well as tourism and education infrastructure (Water Affairs Bureau of Fangshan Beiing 2007). The district has 28 townships, towns, and sub-district offices. The registered population in 2014 was 790,000. A high flood disaster risk has accompanied the district's rapid urbanization and aggregation of population and wealth. From July 21 to 22, 2012, Beijing and the surrounding area suffered the strongest rainstorm since 1961. The Fangshan District was severely damaged by the resulting floods where 38 people died, over 80% of the people were affected, and the direct economic losses were estimated to be over 6.1 billion yuan.

2.2 Data sources

This study used daily precipitation data from 14 rain gauges in the Fangshan District from 2012 to 2015; the data were obtained from the Beijing Water Authority. The Landsat 8 (TM) images of the Beijing area with a spatial resolution of 30 m, which were taken in August 2014, were used to extract ground cover information. The digital elevation model (DEM) was obtained using the elevation data from the Shuttle Radar Topography Mission (SRTM) provided by the National Data Sharing Infrastructure of Earth System Science. These data have a spatial resolution of 90 m. The socioeconomic data (town area, population, and fixed assets) were from the 2014 Statistical Yearbook of the Fangshan District.

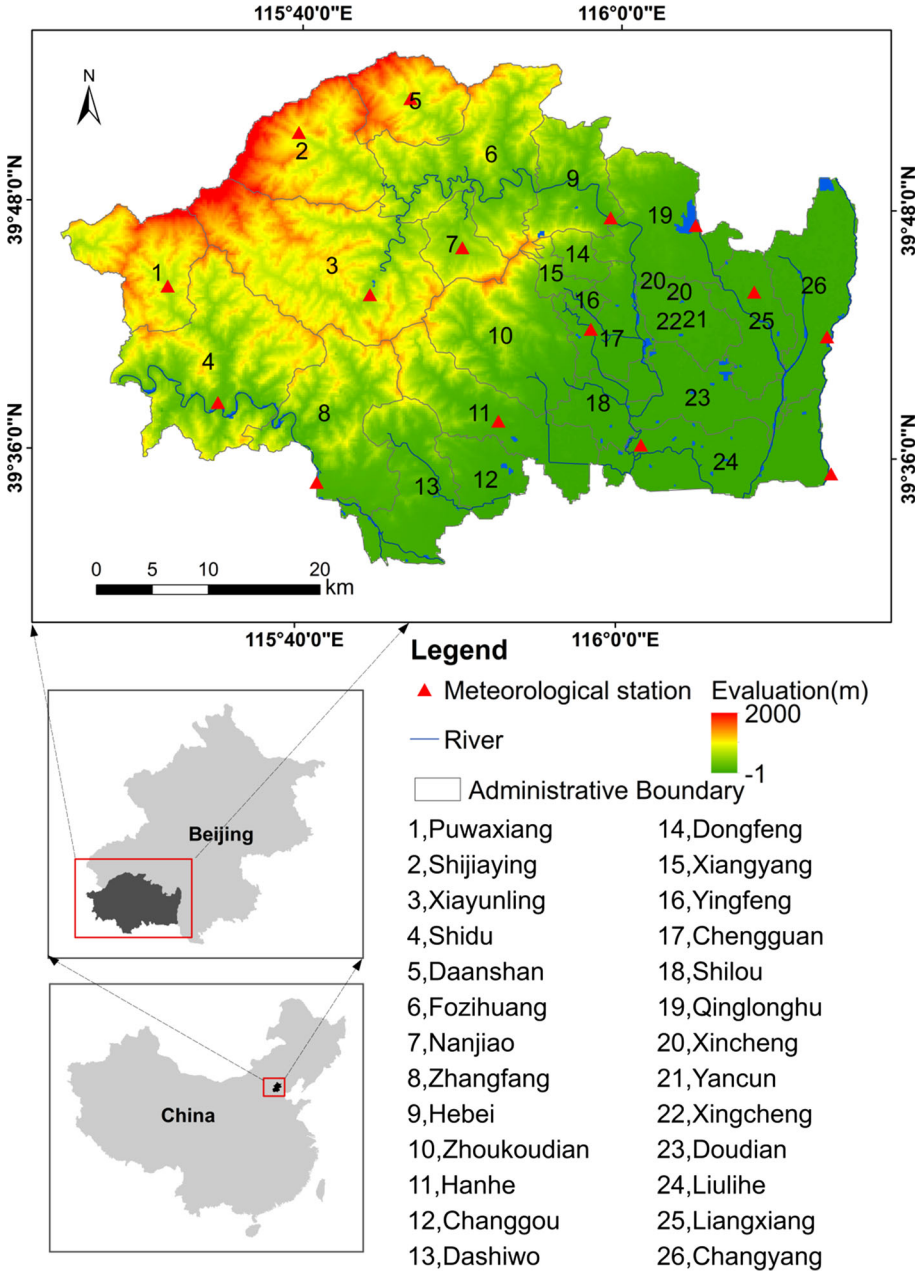

Fig. 1 Location of the Fangshan District

3 Study methodology

3.1 Conceptual model of flood risk assessment

Regional flood disaster system can be characterized as a system that includes disaster-forming environments, disaster-inducing factors, and a hazard-bearing body. The disaster risk can be expressed as the product of interactions between these subsystems (Blaikie et al. 2004). In this study, hazard and vulnerability indices were used to construct a comprehensive assessment index system (Jiang et al. 2008; Zou et al. 2013; Wang et al. 2011). The weight of each index was obtained according to the AHP method, with ArcGIS software as the platform, and 200 × 200 m^2 grids were used as assessment units. The basic process of conducting the risk assessment is as follows: index selection, index quantification, risk calculation, risk analysis, and risk verification. The schematic representation of the evaluation criteria of the flood risk assessment is given in Fig. 2.

3.2 Index selection and extraction

3.2.1 Hazard factors

The hazard of flood disasters is related to the effect of the natural features of the study region and includes both disaster-inducing factors and disaster-forming environments (Yu et al. 2013). High-intensity rainfall over a short period of time is the most important factor that causes flood disasters. In this study, the disaster-inducing factors were rainstorm intensity and rainstorm frequency. Most studies of regional precipitation in China have shown that Kriging interpolation methods can reproduce the spatial distribution pattern of precipitation (Lu et al. 2006; Shao et al. 2006). Therefore, this research adopted the Kriging method to construct grid maps of disaster-inducing indices for the entire area by interpolating rainstorm intensity and rainstorm frequency data from individual stations.

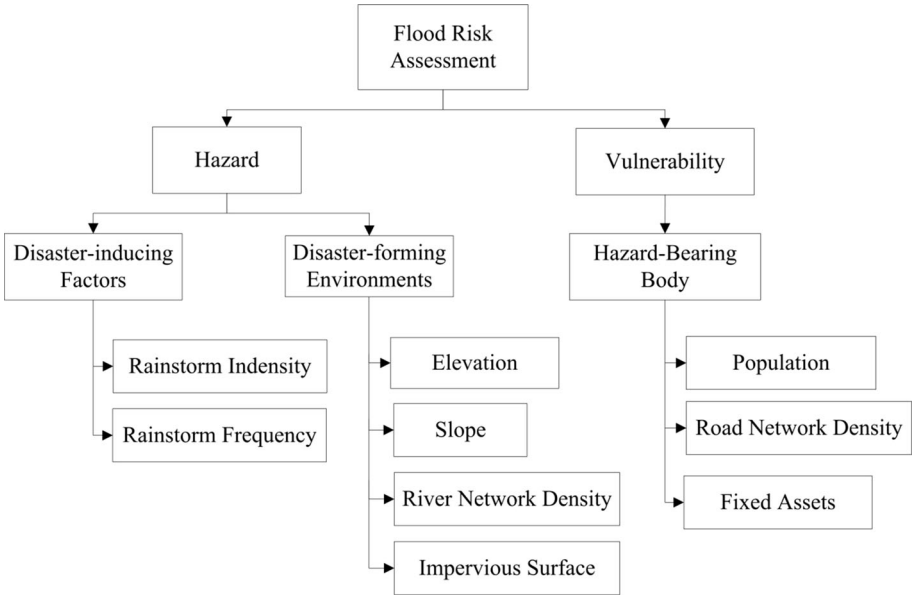

Fig. 2 Hierarchy of flood risk assessment in the Fangshan District

Disaster-forming environments refer to the natural features that determine the effects of rainstorms, including topography, geology, soil, vegetation, slope, and drainage (Li et al. 2012; Zeleňáková et al. 2015). The disaster-forming environments included in this study were elevation, slope, river network density, and the impervious surface ratio. Elevation data were extracted from the DEM by resampling. The slope data were obtained from the DEM using the ArcGIS' surface analysis module. To extract the impervious surface ratio, we obtained impervious surface information using Landsat images during the first step. Next, we used the Zonal Statistics tool in the ArcGIS Spatial Analyst toolbox to calculate the impervious surface area ratio for each grid cell. The extraction process for the river network density is similar to the method of calculating the impervious surface area ratio and involves the following steps (Jiang et al. 2009a, b): (1) Build a grid layer that covers the Fangshan District; (2) perform a spatial overlay with the river layer and grid layer; (3) calculate the river network ratio for each grid cell with the Zonal Statistics tool; and (4) convert the vector data into raster data.

3.2.2 *Vulnerability factors*

Vulnerability is an intrinsic feature of the receptors and indicates the degree to which receptors are susceptible to cope with, resist, and recover from the adverse effects of urban flooding (Yin et al. 2015). Social and economic indices are often used to quantitatively reflect regional vulnerability. This study used vulnerability indices of population, economy, and transportation (Ge et al. 2013). For the vulnerability index of population, this study selected the total population per unit area. For the economic vulnerability index, this study selected the fixed assets per unit area. For the transportation vulnerability index, this study selected the road network density (Ji et al. 2013). The method used to construct the index of road network density is the same as the river network density. The details are given in Sect. 3.2.1. The population and economic indices were spatialized using a spatialization model based on land use. The model is stated through the spatialization of population as follows: Because land use information can reflect minor variations in population, this paper conducted a relevance analysis for the population of each administrative unit and different land use types (Liao and Li 2003). This set up the quantitative relation between land use factors and population distribution based on which the population spatialization model in the Fangshan District is built. Its general form is

$$P_i = \sum_{j}^{n} a_j x_j + B_i \tag{1}$$

where P_i represents the population of the ith administrative unit; a_j indicates the population distribution coefficient of the jth land use type for the ith administrative unit; x_j is the area of the jth land use type for the ith administrative unit; n is the number of land use types that affect the distribution of the population; and B_i is the intercept of the equation, which is set to 0, according to the principle of no land, no population.

The model shown in Eq. (1) is based on the assumption that the land-type distribution coefficient is the same for the same land type. To ensure that the total population in the study area is equal to the actual statistical population (Jin et al. 2014), Eq. (2) is used to adjust the coefficient of the population space model.

$$a_{j'} = \frac{p'}{p} a_j \tag{2}$$

where $a_{j'}$ is the adjusted coefficient; p' indicates the statistical population for the Fangshan District; p is the simulation population; and a_j is the initial coefficient of the population spatial model.

The spatial method of fixed assets is the same as the population; however, the regression coefficient of fixed assets is not adjusted because the constant term exists in the model.

3.3 Index standardization

To compare the indices, all of the indices were made dimensionless. After standardization, the values ranged from 1 to 10, which revealed the effect of each factor on the hazard or vulnerability of flood disasters. For the factors, Eq. (3) is applied to the positive indices, and Eq. (4) is applied to the negative indices.

$$Y = 1 + 9 \times (X - X_{\min})/(X_{\max} - X_{\min}) \tag{3}$$

$$Y = 1 + 9 \times (X_{\max} - X)/(X_{\max} - X_{\min}) \tag{4}$$

where X is the raw data; $X_{\min}$ and $X_{\max}$ are the maximum and minimum values in the data; and Y indicates the standardized value. The final index distribution map for each factor is shown in Fig. 3.

3.4 Factors weight

The AHP is used to determine the weight of each index (Dyer 1990). The main steps are as follows: (1) Establish the hierarchical structure according to the evaluation index system; (2) create the judgment matrix; (3) calculate the weight; (4) perform the consistency test;

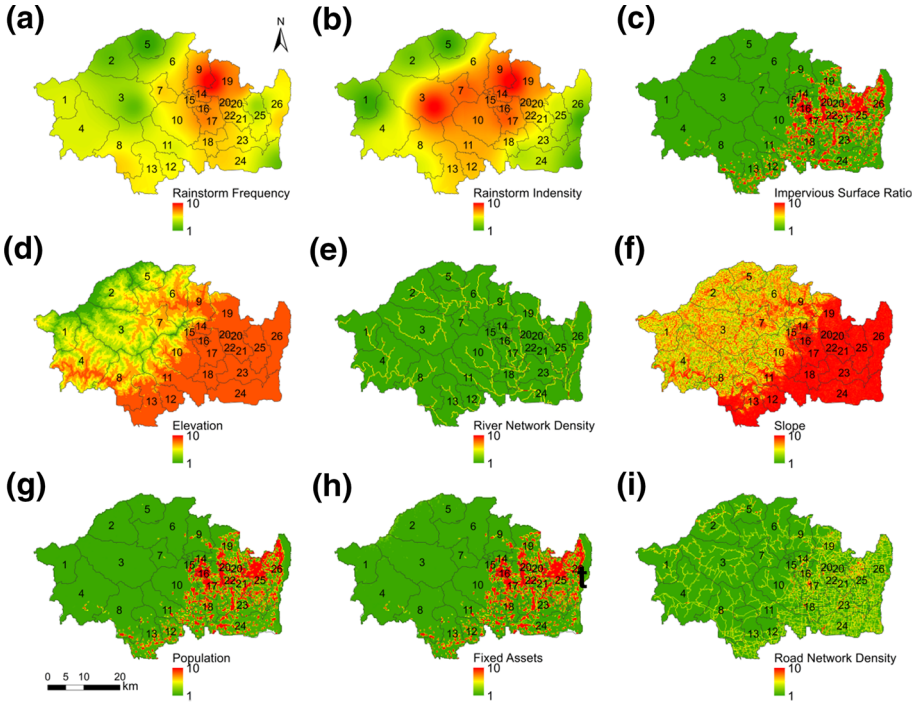

Fig. 3 Index distribution of flood disaster: **a** precipitation frequency index, **b** precipitation intensity index, **c** impervious surface ratio index, **d** elevation index, **e** river network density index, **f** slope index, **g** population index, **h** fixed assets index, **i** road network density index

and (5) calculate the combination weighting of elements at all levels as well as the total consistency test (Chen et al. 2011). The weight determined using this method is shown in Table 1.

3.5 Risk index calculation

According to the weighted comprehensive analysis method, the risk assessment model can be described by (Maskrey 1989; Masood and Takeuchi 2012):

$$R = w_H \times H + w_V \times V \tag{5}$$

where H indicates the hazard; V indicates the vulnerability; and w_H and w_V are the corresponding weights. The hazard is calculated by

$$H = (w_{RZ} \times RI + w_{RF} \times RF) + (w_h \times h + w_{Rh} \times Rh + w_{WD} \times WD + w_{IS} \times IS) \tag{6}$$

where H denotes the hazard; RI, RF, h, Rh, WD, and IS indicate the rainstorm intensity, rainstorm frequency, elevation, slope, river network density, and impervious surface ratio, respectively; and, w_{RZ}, w_{RF}, w_h, w_{Rh}, w_{WD}, and w_{IS} are the weights of each. Vulnerability is calculated by

$$V = w_{POP} \times POP + w_{GDP} \times GDP \tag{7}$$

where V denotes vulnerability, POP and GDP stand for population and fixed assets; w_{POP} and w_{GDP} are the corresponding weights.

Following 3.1–3.5, the flood disaster risk index, the vulnerability index, and the risk index were obtained. The index value range is between 1 and 10, where the higher the index, the greater the risk. In this study, the risk index is divided into five levels: very high, high, medium, low, and very low with the ArcGIS Jenks natural breaks method.

Table 1 Weight of flood risk index

Flood risk indicators	Hazard 0.667		Vulnerability 0.333
	Triggering factors 0.620	Conditions 0.380	
Rainstorm intensity	0.649		
Rainstorm frequency	0.351		
Elevation		0.371	
Slope		0.154	
River network		0.250	
Impervious surface		0.225	
Population			0.400
Fixed assets			0.400
Road network			0.200

4 Results

4.1 Hazard assessment results in the Fangshan District

Using the grid cell data and the determined weight for each of the six flood hazard factors, a distribution of the level of flood disaster hazards in the Fangshan District was obtained (Fig. 4).

Figure 4 shows that the level of flood disaster hazard decreases away from the center of the transition zone between the mountains and plains in the northern part of the Fangshan District. Analyzing the areas and percentages of different hazard grades shows that there is a wide distribution of regions with at least an intermediate hazard, accounting for 1281.5 km^2, or 64.9% of the total area of the Fangshan District. These regions are located primarily in the central to northern parts of the district. The highest hazard regions are in the north-central part of the Fangshan District and account for an area of 207.9 km^2, or 10.5% of the total area of the district. The areas of intermediate hazard and the second highest hazard regions are distributed in a circular pattern surrounding the highest hazard regions. The two areas account for 601.2 and 472.4 km^2, respectively. The second lowest hazard and lowest hazard regions are concentrated near the western mountains and along the southeastern edge of the Fangshan District.

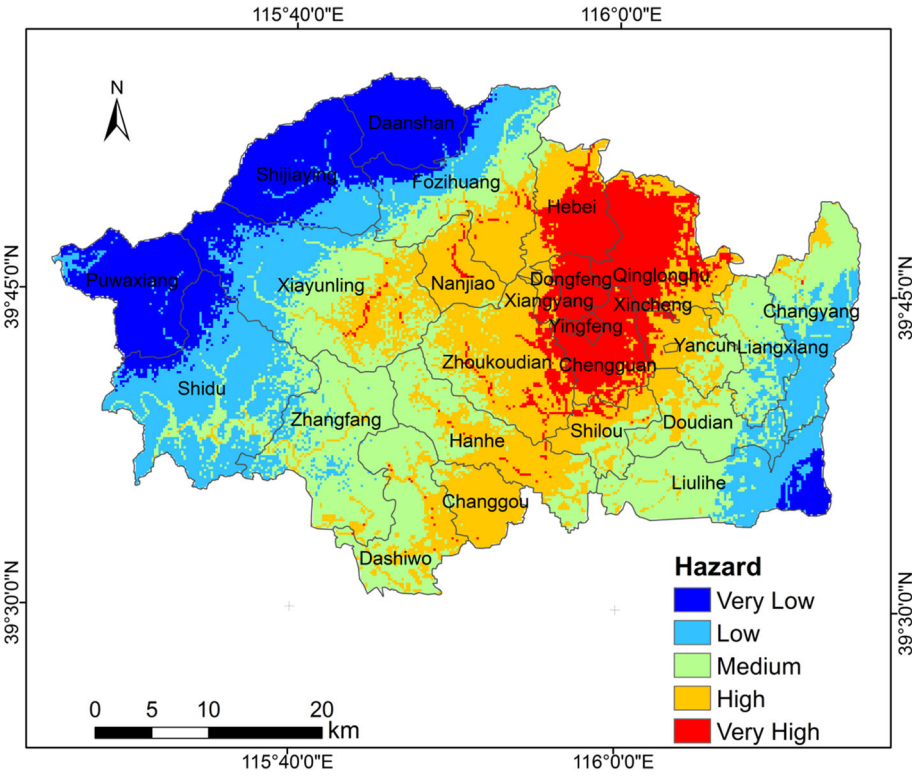

Fig. 4 Hazard distribution map in the Fangshan District

In terms of administrative divisions (Table 2), the regions of relatively high levels of flood hazards are located primarily in the district's central city and along the boundary between the towns of Hebei and Qinglonghu in the north, for which the second highest and highest flood hazard areas account for 99.9 and 95.0%, respectively. These regions are mostly characterized by piedmont plains with flatter topography compared with that of the mountain regions, where rainstorms are common. In addition to that, these regions are mostly urban areas that include large amounts of impervious surfaces (Fig. 3c), which favors rainwater convergence. The regions of relatively low levels of hazard include the Da'anshan Township, the Shijiaying Township, and the Puwa Township, all of which are in the western mountains. Among them, the hazard level of Da'anshan is the lowest, where the very low hazard areas account for 95.8% of the total area. The elevation variation in these regions is large, and the vegetation coverage is high, which favors rainwater dispersion and storage. In addition, the rainstorm frequency (Fig. 3a) and intensity (Fig. 3b) are lower, which leads to lower hazard levels.

Table 2 Hazards statistics for each administrative division

District	Hazards coverage (%)				
	Very low	Low	Medium	High	Very high
Yingfeng	0.0	0.0	0.0	1.8	98.2
Dongfeng	0.0	0.0	0.0	9.7	90.3
Hebei	0.0	0.0	0.1	36.0	63.9
Xiangyang	0.0	0.0	0.0	40.6	59.4
Qinglonghu	0.0	0.2	4.8	44.2	50.8
Chengguan	0.0	0.0	1.5	56.7	41.9
Nanjiao	0.0	0.0	0.6	80.1	19.3
Xincheng	0.0	0.0	2.0	81.6	16.3
Zhoukoudian	0.0	0.0	10.1	80.6	9.3
Fozizhuang	4.2	25.2	36.6	30.7	3.4
Yancun	0.0	10.9	53.5	33.8	1.9
Xiayunling	0.0	25.0	28.8	44.4	1.7
Shilou	0.0	13.5	62.7	23.2	0.6
Hanhecun	0.0	1.2	62.5	36.2	0.1
Xingcheng	0.0	0.0	11.5	88.5	0.0
Zhangfang	0.0	5.2	72.9	21.9	0.0
Changgou	0.0	0.0	87.5	12.5	0.0
Dashiwo	0.0	2.1	88.8	9.1	0.0
Doudian	6.1	50.4	38.9	4.7	0.0
Shidu	5.2	42.6	50.6	1.6	0.0
Changyang	29.8	53.4	16.2	0.7	0.0
Liangxiang	5.7	70.1	23.9	0.3	0.0
Liulihe	38.6	48.7	12.6	0.1	0.0
Shijiaying	50.1	44.0	5.9	0.0	0.0
Puwa	58.9	41.0	0.2	0.0	0.0
Da'anshan	95.8	4.2	0.0	0.0	0.0

4.2 Vulnerability assessment results in the Fangshan District

Figure 5 shows the vulnerability assessment results in the Fangshan District. Overall, the vulnerability to flood disasters in the Fangshan District is low. The regions with the lowest and second lowest vulnerability account for 1309.9 and 332.4 km^2, respectively, or 66.0 and 16.8% of the administrative area of the Fangshan District. The region with the highest vulnerability accounts for 174.9 km^2, or 8.8% of the area of the district. These areas are distributed on either side of the boundary between the mountains and the plains, with the lowest vulnerability regions concentrated in the western mountains and the highest vulnerability regions concentrated in the eastern plain regions.

In terms of administrative divisions (Table 3), the highest vulnerability regions include Yingfeng Street, Xingcheng Street, Xincheng Street, and the Liangxiang region, as well as the Yancun region; for all of these regions, the percentage of area characterized by the second highest and highest vulnerability exceeds 50%. The Twelfth Five-Year Plan of the Fangshan District puts forward an urbanization strategy that is concentrated on building two new town centers in Liangxiang and Changyang, as well as in Yanfang (including Dongfeng Street, Xiangyang Street, Yinfeng Street, and Chengguanzhen Street). The plan also focuses on the urban communities of Doudian, Liulihe, Changgou, and Hebei. This has led to much greater urbanization in these areas. Thus, population aggregation and economic development are high in these regions, leading to potentially high losses from flood disasters. Therefore, their flood vulnerability is relatively high. The vulnerability

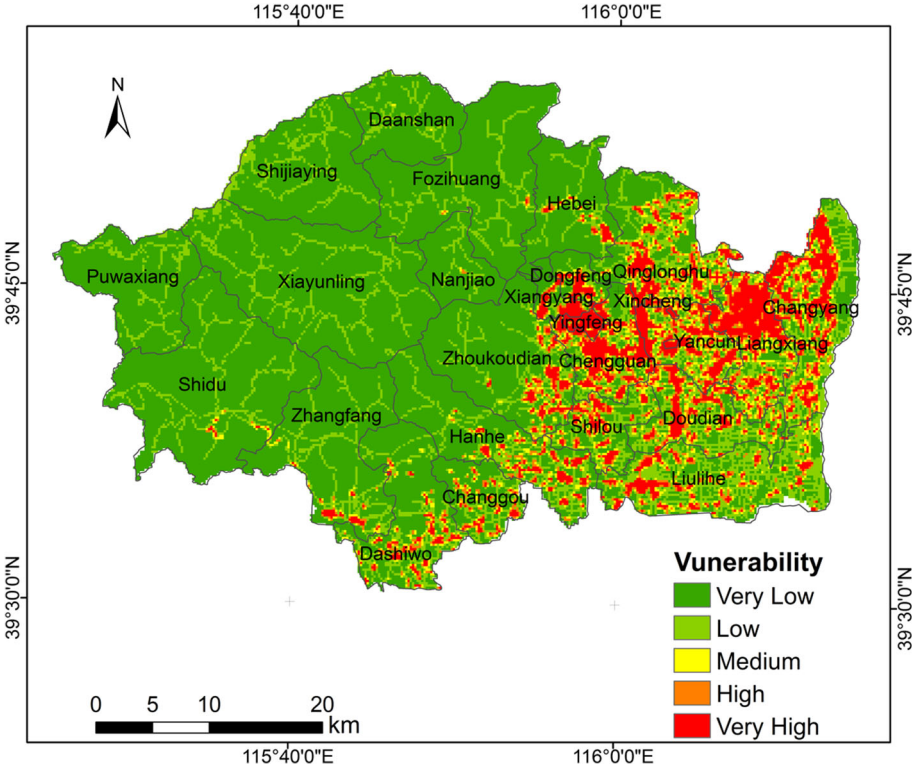

Fig. 5 Vulnerability distribution map in the Fangshan District

Table 3 Vulnerability statistics for each administrative division

District	Vulnerability coverage (%)				
	Very low	Low	Medium	High	Very high
Yingfeng	0.0	1.4	2.8	2.8	93.0
Xingcheng	0.0	0.0	5.0	5.0	90.0
Xincheng	4.3	10.9	6.5	13.0	65.2
Liangxiang	12.4	16.9	13.0	12.5	45.2
Chengguan	21.7	19.0	11.7	9.7	37.9
Yancun	10.7	22.6	16.3	14.3	36.0
Xiangyang	45.8	10.9	3.9	6.1	33.2
Changyang	24.3	26.6	10.3	10.4	28.4
Dongfeng	55.2	10.9	6.7	5.7	21.4
Doudian	25.5	33.3	11.4	10.6	19.2
Qinglonghu	39.4	24.7	10.4	8.6	16.8
Shilou	35.6	29.4	10.3	9.1	15.6
Liulihe	30.5	44.4	7.6	7.0	10.5
Hanhecun	65.8	18.1	5.3	4.3	6.6
Changgou	55.2	23.5	6.3	8.7	6.3
Zhoukoudian	74.8	12.4	3.6	3.5	5.8
Dashiwo	64.3	19.7	5.9	4.5	5.6
Hebei	84.3	9.5	1.7	1.7	2.8
Zhangfang	83.3	12.6	1.5	1.0	1.6
Shidu	91.4	7.5	0.6	0.2	0.2
Fozizhuang	92.3	7.3	0.2	0.2	0.1
Nanjiao	91.9	7.6	0.2	0.3	0.0
Da'anshan	88.8	11.0	0.1	0.0	0.0
Shijiaying	86.2	13.8	0.0	0.0	0.0
Xiayunling	89.7	10.3	0.0	0.0	0.0
Puwa	90.0	10.0	0.0	0.0	0.0

statistics for each administrative division (Table 3) can also reflect the degree of urbanization in these regions. The larger the proportion of the highest and second highest vulnerability areas, the higher the degree of urbanization. In contrast to the regions with the highest vulnerability, the regions with the lowest vulnerability are concentrated in the Xiayunling Township, the Shidu Township, and the Puwa Township to the west, where the economy is underdeveloped, and the primary objective is ecological protection.

4.3 Comprehensive risk assessment results in the Fangshan District

Figure 6 shows the comprehensive risk assessment results in the Fangshan District. The total area of the regions with the highest and second highest risk of flood disasters is 441.3 km^2, or 22.4% of the area of the district. The highest risk is concentrated in the Dashi, Xisha, and Dongsha River areas. The regions with the second highest risk are mostly upstream of the Dashi River area and near the Ciwei and Xiaoqing River areas. The areas subject to intermediate risk account for 692.0 km^2 and are concentrated in the central part of the Fangshan District. The areas of the regions with the lowest and second lowest

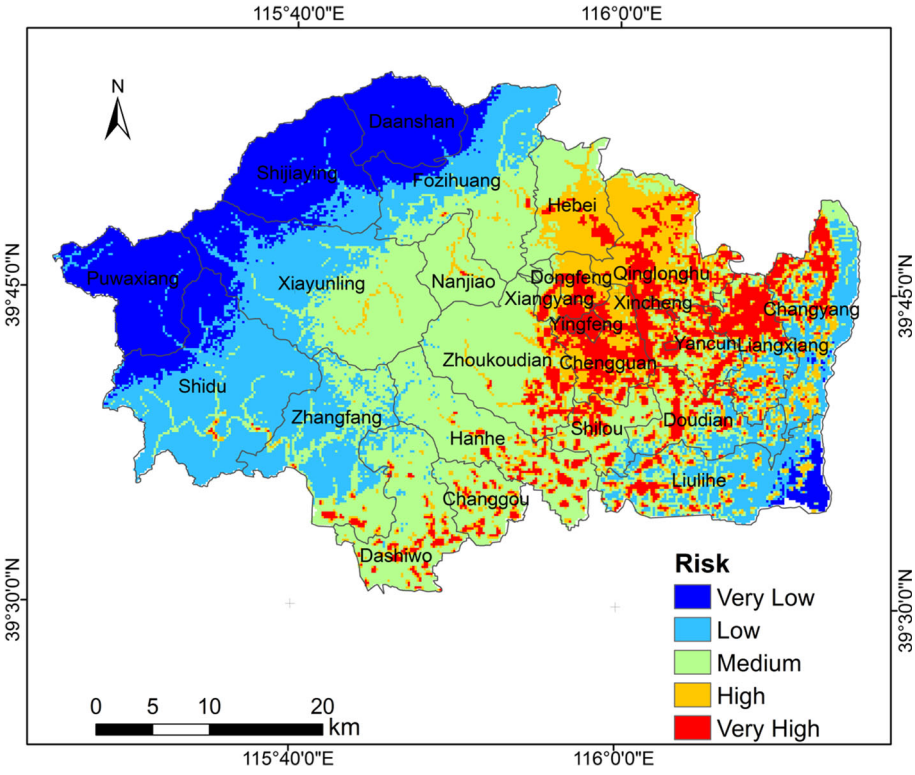

Fig. 6 Risk of flood disaster in the Fangshan District

risks are 339.9 and 498.1 km^2, respectively, constituting 17.2 and 25.3% of the area of the Fangshan District.

In terms of administrative divisions (Table 4), the regions with the highest rainstorm and flood disaster risk are Yingfeng Street, Xingcheng Street, Xincheng Street, and Chengguanzhen Street, whose total areas that belong to the second highest and highest comprehensive risk exceed 90%. These areas are in the plains and have a flat topography and a concentrated river network; thus, they are prone to flood disasters during intense precipitation events. In addition, because the central and eastern plain regions include the population and economic center of the Fangshan District, the vulnerability of a hazard-bearing body in these regions is more obvious. Therefore, their comprehensive risk grade is high. The regions with intermediate risk are located in the eastern part of the town of Hebei and the northwestern Qinglonghu area. These regions are in the transition zone between the mountains and plains, and their elevation and population density are low; however, these regions experience high rainstorm intensities. Therefore, their flood risk is intermediate between the eastern plains and the western mountains. The low-risk regions are concentrated in the western mountains, where there are underdeveloped economies and low population densities. These regions include the Da'anshan Township, the Puwa Township, and the Shijiaying Township. The total area that belongs to the "very low" risk class in these regions is 80%.

Table 4 Comprehensive risk statistics for each administrative division

District	Comprehensive risk coverage (%)				
	Very low	Low	Medium	High	Very high
Yingfeng	0.0	0.0	0.0	4.3	95.7
Xingcheng	0.0	0.0	0.0	9.1	90.9
Xincheng	0.0	0.0	9.3	14.0	76.7
Chengguan	0.0	0.0	8.7	41.3	50.0
Yancun	0.0	2.8	29.1	25.7	42.4
Liangxiang	0.0	20.5	17.4	21.3	40.9
Xiangyang	0.0	0.0	37.7	22.5	39.7
Dongfeng	0.0	0.0	5.7	63.3	31.0
Qinglonghu	0.0	0.0	14.4	57.6	28.0
Shilou	0.0	5.0	57.0	17.2	20.8
Changyang	0.8	38.9	18.9	21.3	20.1
Doudian	0.0	26.0	36.8	17.6	19.6
Changgou	0.0	0.4	75.1	13.8	10.7
Zhoukoudian	0.0	0.4	79.0	11.5	9.1
Hanhecun	0.0	2.5	79.4	9.1	9.1
Liulihe	12.3	45.6	22.5	11.9	7.7
Dashiwo	0.0	6.8	77.0	8.6	7.5
Hebei	0.0	0.5	45.9	46.9	6.7
Zhangfang	0.0	51.8	44.2	2.3	1.7
Nanjiao	0.0	0.0	93.8	5.8	0.4
Fozizhuang	12.4	45.7	40.1	1.6	0.3
Shidu	19.8	74.0	5.3	0.6	0.2
Xiayunling	16.3	39.3	43.1	1.2	0.0
Shijiaying	82.4	17.5	0.1	0.0	0.0
Puwa	96.4	3.6	0.0	0.0	0.0
Da'anshan	99.4	0.6	0.0	0.0	0.0

4.4 Verification and assessment

Due to a lack of detailed data on disaster damage in the study area, the casualty distribution map of the Beijing flood disaster on July 21, 2012, was used to verify the flood risk obtained in this study. It is assumed that the population death sites accurately reflect the high-risk area of a flood disaster. We overlaid the vector layer of casualties in the July 21 rainstorm onto the flood disaster risk map and summarized the casualties in regions of each grade (Fig. 7). It was found that the 38 casualties in the July 21 rainstorm occurred in a total of 25 locations. A total of 34 casualties occurred in regions with the second highest and highest risk grades, accounting for 89.4% of the total number of casualties. This result is consistent with our results, which indicates that our risk assessment of rainstorm and flood disasters in the Fangshan District matches the actual distribution of risk and thus has a high practical value.

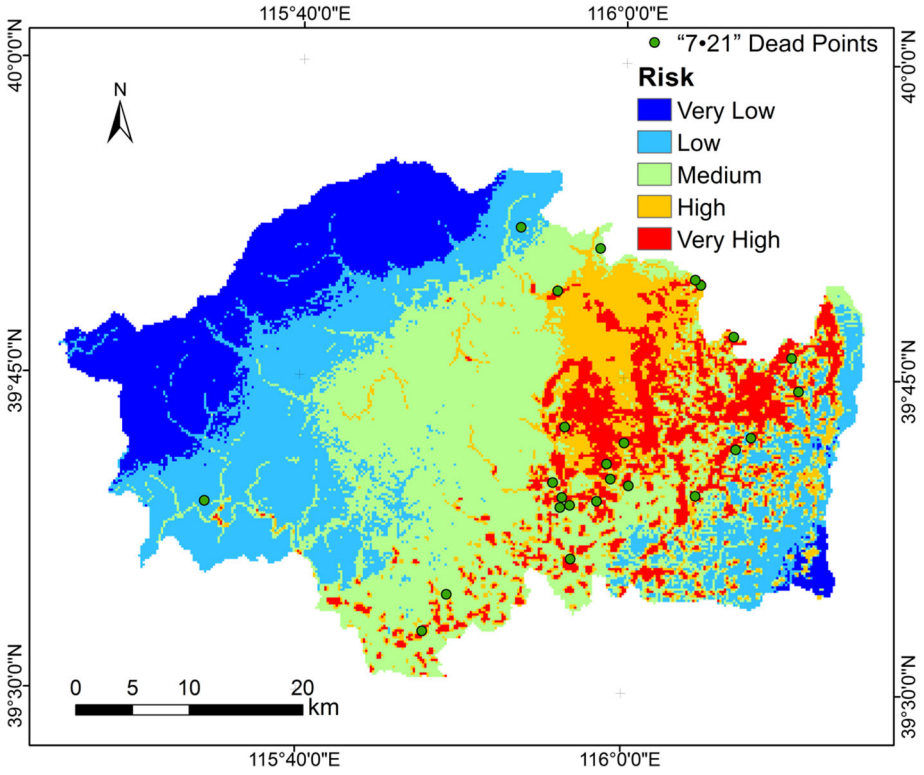

Fig. 7 Verification of the flood disaster risk

5 Discussion

5.1 Implications

Flood risk assessment gives a clear indication of areas that are safe and non-safe for urban development. Therefore, the flood risk map provides valuable information for land use planning and targeting areas for prioritizing risk reduction measures (Alexander et al. 2016; Müller 2013; Abuzied et al. 2016). According to the Fangshan New Town Plan 2005–2020, the categories of urbanization in the Fangshan District are divided into three grades: new towns, key towns, and normal towns (People's Government of Fangshan District 2005). A comparison between the flood disaster risk map and the planned map of new towns in Fangshan (Fig. 8) shows that the Yanfang region (containing Dongfeng Street, Xiangyang Street, and Yingfeng Street) is subject to a high flood risk. Among the three sub-areas, over 90% of Dongfeng Street and Yingfeng Street belong to the second highest and highest flood risk areas (Table 4). This suggests that flood control measures should be increased for urban construction in this area to mitigate flood disaster losses. Doudian, Hanhecun, Liulihe, and Changgou are in the eastern plain region and have low flood risks. As the key development towns in the plan, they have high development potential. The western mountain region is largely characterized by low flood risks and high ecological value. It is reasonable for the plan to designate this region as an ecological

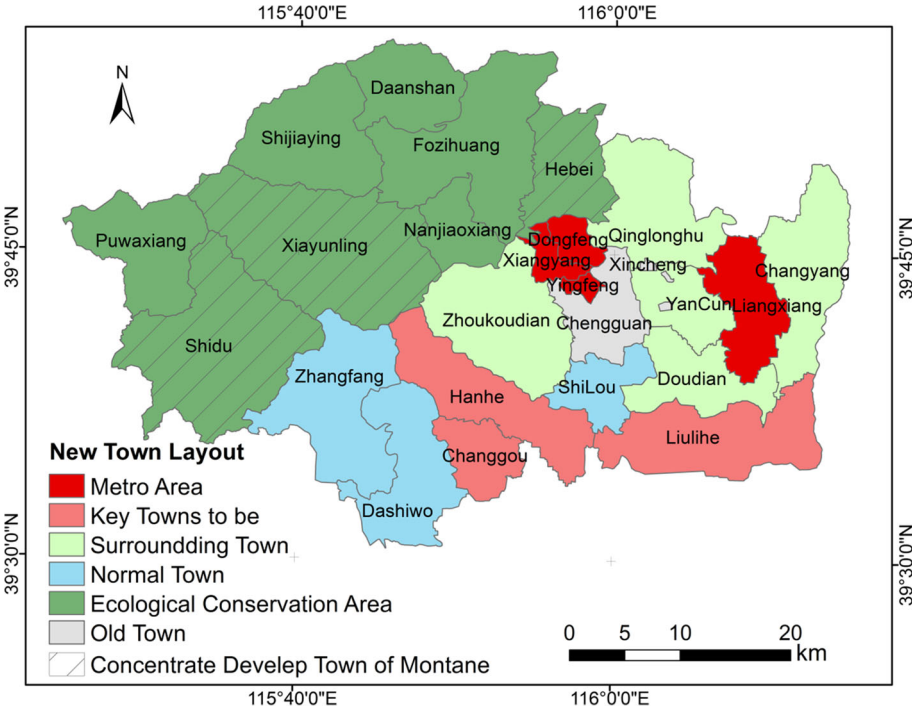

Fig. 8 New town planning of the Fangshan District in 2005–2020

recovery zone, with Shidu, Xiayunling, and Hebei among them as focused development towns in the mountain region. It should be noted that 53.6% of Hebei is characterized as the regions with the second highest and highest flood risk, which should be taken into account during development.

The flood risk map can also offer insurance policy maker information for determining the flood protection capacity according to their tolerance of risk (Hsu et al. 2011). Moreover, flood risk mapping can be used as a tool for increasing awareness on flooding in communities (Alphen et al. 2009).

5.2 Uncertainties

There are many types of uncertainties in flood risk assessment processes. Because a real flood disaster system is complicated and fuzzy, the present assessment model may not fully express the true situation. In this study, the index system considered only nine indexes associated with flood risk. Beyond that, the weight of each index during assessment is partly based on expert experience, which will be impacted by subjective human decisions. In addition, the lack of abundant long-term precipitation data and high-resolution social and economic statistics is another important uncertain factor.

6 Conclusions

This study used the Fangshan District as a case study for flood risk assessment in suburban areas that integrated the use of AHP and GIS. Nine influencing factors were identified as necessary for flood risk assessment, including rainstorm intensity, rainstorm frequency, elevation, slope, river network density, road network density, impervious surface ratio, population, and fixed assets. The major findings are summarized as follows:

1. The proposed methodology showed that 23.9 and 10.5% of the areas belong to "high" and "very high" hazard classes, respectively. The regions of relatively high levels flood hazards are primarily located in the area along the boundary between the towns of Hebei and Qinglonghu in the northern part of the Fangshan District. These regions are mostly characterized by piedmont plains with a flatter topography and are mostly urban areas that include large amounts of impervious surfaces.
2. The percentages of regions that belong to "high" and "very high" vulnerability classes are 4.0 and 8.8%, respectively, and are primarily located on Yingfeng Street, Xingcheng Street, Xincheng Street, and the Liangxiang region, as well as the Yancun region, where the population is concentrated and the economy is well developed.
3. Combining the hazard and vulnerability factors, the total area of the regions with the highest and second highest risks of flood disasters is 441.3 km^2, or 22.4% of the Fangshan District. The regions with the highest rainstorm and flood disaster risk occur in the southern Yanshan area, the central part of the town of Chengguan, the northern Liangxiang area, and the northern part of the town of Changyang.
4. The results are consistent with the historical records of flood disaster distributions, which validate the reliability and applicability of the proposed methodology.

Acknowledgements This research was financially supported by National Natural Science Foundation of China (No. 41501027) and a fund from National Disaster Reduction Center of China (No. NDRCCPICC201403).

References

Abuzied S, Yuan M, Ibrahim S, Kaiser M, Saleem T (2016) Geospatial risk assessment of flash floods in Nuweiba area, Egypt. J Arid Environ 133:54–72. doi:10.1016/j.jaridenv.2016.06.004

Al-Abadi AM, Shahid S, Al-Ali AK (2016) A GIS-based integration of catastrophe theory and analytical hierarchy process for mapping flood susceptibility: a case study of Teeb area, Southern Iraq. Environ Earth Sci 75(8):1–19. doi:10.1007/s12665-016-5523-7

Alexander M, Priest S, Mees H (2016) A framework for evaluating flood risk governance. Environ Sci Policy 64:38–47. doi:10.1016/j.envsci.2016.06.004

Alfieri L, Burek P, Feyen L, Forzieri G (2015) Global warming increases the frequency of river floods in Europe. Hydrol Earth Syst Sc 12(1):1119–1152. doi:10.5194/hessd-12-1119-2015

Alphen JV, Martini F, Loat R, Slomp R, Passchier R (2009) Flood risk mapping in Europe, experiences and best practices. J Flood Risk Manag 2(4):285–292

Ayalew L (2009) Analyzing the effects of historical and recent floods on channel pattern and the environment in the Lower Omo basin of Ethiopia using satellite images and GIS. Environ Geol 58(8):1713–1726. doi:10.1007/s00254-008-1671-8

Blaikie P, Cannon T, Davis I, Wisner B (2004) At risk: natural hazards, people's vulnerability and disasters. Routledge 8(2). doi:10.4324/9780203428764

Camarasa-Belmonte AM, Soriano-García J (2012) Flood risk assessment and mapping in peri-urban Mediterranean environments using hydrogeomorphology. Application to ephemeral streams in the Valencia region (eastern Spain). Landsc Urban Plan 104(2):189–200. doi:10.1016/j.landurbplan.2011.10.009

Chen Y, Yeh C, Yu B (2011) Integrated application of the analytic hierarchy process and the geographic information system for flood risk assessment and flood plain management in Taiwan. Nat Hazards 59:1261–1276. doi:10.1007/s11069-011-9831-7

Dyer JS (1990) Remarks on the analytic hierarchy process. Manage Sci 36(3):249–258

Elkhrachy I (2015) Flash Flood Hazard Mapping Using Satellite Images and GIS Tools: a case study of Najran City, Kingdom of Saudi Arabia (KSA), Egypt. J Rem Sens Space Sci 18(2):261–278. doi:10.1016/j.ejrs.2015.06.007

Ge Y, Dou W, Gu Z, Qian X, Wang J, Xu W, Shi P, Ming X, Zhou X (2013) Assessment of social vulnerability to natural hazards in the Yangtze River Delta, China. Stoch Environ Res Risk Assess 27(8):1899–1908. doi:10.1007/s00477-013-0725-y

Hsu WK, Huang PC, Chang CC, Chen CW, Hung DM, Chiang WL (2011) An integrated flood risk assessment model for property insurance industry in Taiwan. Nat Hazards 58(3):1295–1309. doi:10.1007/s11069-011-9732-9

Islam MM, Sado K (2000) Flood hazard assessment in Bangladesh using NOAA AVHRR data with geographical information system. Hydrol Process 14(3):605–620

Ji Z, Li N, Xie W, Wu J, Zhou Y (2013) Comprehensive assessment of flood risk using the classification and regression tree method. Stoch Environ Res Risk Assess 27(8):1815–1828. doi:10.1007/s00477-013-0716-z

Jiang WG, Jing LI, Yun-Hao C, Sheng SX, Zhou GH (2008) Risk assessment system for regional flood disaster (I):principle and method. J Nat Disasters 17(6):53–59

Jiang LL, Qi Q, Zhang Z, Han J, Cheng X, Zhang A (2009) The abstraction method research of river network based on catchments' characters deriving digital elevation data. Proc SPIE-Int Soc Opt Eng 7146. doi:10.1117/12.813189

Jiang W, Deng L, Chen L, Wu J, Li J (2009b) Risk assessment and validation of flood disaster based on fuzzy mathematics. Prog Nat Sci 19(10):1419–1425. doi:10.1016/j.pnsc.2008.12.010

Jin YJ, Zeng Y, Qiu XF (2014) Vulnerability analysis of flood disasters hazard-affected body under the support of spatialization technology of population and GDP. J Meteorol Sci 34(5):522–529. doi:10.3969/2013jms.0030

Lai C, Chen X, Chen X, Wang Z, Wu X, Zhao S (2015) A fuzzy comprehensive evaluation model for flood risk based on the combination weight of game theory. Nat Hazards 77(2):1243–1259. doi:10.1007/s11069-015-1645-6

Li XC, Bai ML, Yang J, Di RQ, Gao ZG (2012) Risk zonation and evaluation of rainstorm and flood disasters in Inner Mongolia based on GIS. J Arid Land Resour Environ 26(7):71–77

Liao SB, Li ZH (2003) Study on spatialization of population census data based on relationship between population distribution and land use-taking Tibet as an example. J Nat Res 18(6):659–665

Liao S, Sun J (2003) GIS based spatialization of population census data in Qinghai-Tibet Plateau. Acta Geogr Sin 58(1):25–33

Liu X, Luo Y, Zhang D, Zhang M, Liu C (2011) Recent changes in pan-evaporation dynamics in China. Geophys Res Lett 38:142–154. doi:10.1029/2011GL047929

Liu X, Song Y, Wu K, Wang J, Li D, Long Y (2015) Understanding urban China with open data. Cities 47:53–61. doi:10.1016/j.cities.2015.03.006

Lu ZY, Yang TB, Guo WQ (2006) Application of the spatial interpolation of rainfall–a case study of the headstream region of the yellow river. J Lanzhou Univ 42(4):11–14 **(in Chinese)**

Maskrey A (1989) Disaster mitigation: a community based approach. Oxfam, Oxford

Masood M, Takeuchi K (2012) Assessment of flood hazard, vulnerability and risk of mid-eastern Dhaka using Dem and 1D hydrodynamic model. Nat Hazards 61(61):757–770. doi:10.1007/s11069-011-0060-x

Müller A (2013) Flood risks in a dynamic urban agglomeration: a conceptual and methodological assessment framework. Nat Hazards 65(3):1931–1950. doi:10.1007/s11069-012-0453-5

People's Government of Fangshan District (2005) New Town planning of Fangshan for 2005–2020, Beijing (**in Chinese**)

Ranger N, Hallegatte S, Bhattacharya S, Bachu M, Priya S, Dhore K, Rafique F, Mathur P, Naville N, Henriet F (2011) An assessment of the potential impact of climate change on flood risk in Mumbai. Clim Change 104(1):139–167. doi:10.1007/s10584-010-9979-2

Shao XM, Yan CR, Wei HB (2006) Spatial and temporal structure of precipitation in the yellow river basin based on kriging method. Chin J Agrometeorol 27(2):65–69 **(in Chinese)**

Siddayao GP, Valdez SE, Fernandez PL (2014) Analytic hierarchy process (AHP) in spatial modeling for floodplain risk assessment. J Mach Learn Res 4(5):450–457. doi:10.7763/IJMLC.2014.V4.453

Skakun S, Kussul N, Shelestov A, Kussul O (2014) Flood hazard and flood risk assessment using a time series of satellite images: a case study in Namibia. Risk Anal 34(8):1521–1537. doi:10.1111/risa.12156

Tullos D, Byron E, Galloway G, Obeysekera J, Prakash O, Sun YH (2016) Review of challenges of and practices for sustainable management of mountain flood hazards. Nat Hazards 83(3):1–35. doi:10.1007/s11069-016-2400-3

Vorogushyn S, Lindenschmidt KE, Kreibich H, Apel H, Merz B (2012) Analysis of a detention basin impact on dike failure probabilities and flood risk for a channel-dike-floodplain system along the river Elbe, Germany. J Hydrol s 436–437(3):120–131

Wang Y, Li Z, Tang Z, Zeng G (2011) A GIS-based spatial multi-criteria approach for flood risk assessment in the Dongting Lake Region, Hunan, Central China. Water Resour Manag 25(13):3465–3484. doi:10.1007/s11269-011-9866-2

Water Affairs Bureau of Fangshan Beiing (2007) Comprehensive planning of water resources in Fangshan District of Beijing, Beijing (**in Chinese**)

Wells JA, Wilson KA, Abram NK, Nunn M, Gaveau DLA, Runting RK, Tarniati N, Mengersen KL, Meijaard E (2016) Rising floodwaters: mapping impacts and perceptions of flooding in Indonesian Borneo. Environ Res Lett 11(6):64016. doi:10.1088/1748-9326/11/6/064016

Wu Y, Zhong P, Zhang Y, Xu B, Ma B, Yan K (2015) Integrated flood risk assessment and zonation method: a case study in Huaihe River basin, China. Nat Hazards 78:635–651. doi:10.1007/s11069-015-1737-3

Yang N (2013) Approach of county population statistical data spatialization based on GIS. Geospatial Inf (**in Chinese**). doi:10.11709/j.issn.1672-4623.2013.05

Yang XL, Ding JH, Hou H (2013) Application of a triangular fuzzy AHP approach for flood risk evaluation and response measures analysis. Nat Hazards 68(2):657–674. doi:10.1007/s11069-013-0642-x

Yin J, Ye M, Yin Z, Xu S (2015) A review of advances in urban flood risk analysis over China. Stoch Environ Res Risk Assess 29(3):1063–1070. doi:10.1007/s00477-014-0939-7

Yu MJ, Xu YP, Wang LY (2013) Analysis of flood risk of small and medium-sized river basins in southeast China under the impacts of urbanization: a case study of Yongcaopu area. J Nat Disasters 22(4):108–113

Zare M (2016) Integrating Spatial Multi Criteria Decision Making (SMCDM) with Geographic Information Systems (GIS) for determining the most suitable areas for artificial groundwater recharge, vol 45. Iahr Europe Congress

Zeleňáková M, Gaňová L, Purcz P, Satrapa L (2015) Methodology of flood risk assessment from flash floods based on hazard and vulnerability of the river basin. Nat Hazards 79(3):2055–2071. doi:10.1007/s11069-015-1945-x

Zeng F, Lai C, Wang Z (2012) Flood risk assessment based on principal component analysis for Dongjiang River Basin. In: International conference on remote sensing

Zhou H, Zhang D (2009) Assessment model of drought and flood disasters with variable fuzzy set theory. Trans Chin Soc Agric Eng 25(9):56–61(**in Chinese**). doi:10.3969/j.issn.1002-6819.2009.09.010

Zou Q, Zhou J, Zhou C, Song L, Guo J (2013) Comprehensive flood risk assessment based on set pair analysis-variable fuzzy sets model and fuzzy AHP. Stoch Environ Res Risk Assess 27(2):525–546. doi:10.1007/s00477-012-0598-5